J. exp. Biol. ***196***, *419–438 (1994)*
Printed in Great Britain © The Company of Biologists Limited 1994

ENDOSOMAL ACCUMULATION OF pH INDICATOR DYES DELIVERED AS ACETOXYMETHYL ESTERS

CLIFFORD L. SLAYMAN, VASILIANA V. MOUSSATOS

Department of Cellular and Molecular Physiology, Yale School of Medicine, 333 Cedar Street, New Haven, CT 06510, USA

AND WATT W. WEBB

School of Applied and Engineering Physics, Developmental Resource for Biophysical Imaging and Opto-electronics, Cornell University, Ithaca, NY 14852, USA

Summary

Intracellular distributions of the putative cytosolic pH indicator dyes BCECF [2′,7′-bis-(2-carboxyethyl)-5(and 6)-carboxyfluorescein], C.SNARF [5(and 6)-carboxy-seminaphthorhodafluor-1], and C.SNARF-calcein have been examined in *Neurospora crassa* and in murine fibroblasts (NIH-3T3 cells) under conditions in which both kinds of cells produce visible microscopic vacuoles. All three dyes were administered in electroneutral forms, with the hydroxyl and carboxyl groups esterified (designated as -AM esters). As judged qualitatively from fluorescence levels, hydrolytic derivatives of the two heavily esterified dyes (BCECF-AM and C.SNARF-calcein-AM) accumulated in the vacuoles after exposures of approximately 15 min or more, while the simpler dye (C.SNARF-AM) and its derivatives were almost excluded from visible vacuoles. Fluorescence from this dye, alone among the three, also washed out of *Neurospora* rapidly upon removal of extracellular dye. There was no evidence for stable accumulation of any of the dyes in cytosol *per se*. For BCECF(-AM), comparison of the distribution of fluorescence with the size distribution of vacuoles in *Neurospora* strongly suggests that the dyes are also accumulated by endomembranal vesicles (EMVs) which lie below the limit of resolution in the light microscope, and the same inference can be drawn for the fibroblasts. Uptake of -AM dyes by EMVs, including frank vacuoles, probably results from the action of intravesicular esterases, following diffusional entry of lipophilic neutral molecules or partially de-esterified anions. Calculations of actual cytosolic pH values, or even changes of pH, based on intracellular fluorescence of these dyes, clearly depend upon quantitative knowledge of the subcellular dye distribution. Therefore, until the problem is reliably solved of how to visualize submicroscopic vesicles in living cells, the safest approach to the use of BCECF, C-SNARF and their congeners for cytosolic pH measurement would be to devise methods for coaxing uptake of the ionic forms of these dyes and to abandon use of the esterified forms.

Introduction

The predominant mechanism for concentrative uptake of most nutrients by plants, fungi

Key words: BCECF-AM, SNARF-AM, vacuoles, endosomes, lysosomes, *Neurospora crassa*, fibroblasts, confocal microscope.

and many bacteria is symport with protons, drawing upon the transmembrane electrochemical gradient of H^+ to build finite countergradients of sugars, amino acids, inorganic ions, nucleotide precursors, etc. And indeed, over the past 6–8 years, molecular biological techniques have led to the cloning and sequencing of large numbers of these symport systems (Quagliariello and Palmieri, 1992; Friedlander and Mueckler, 1992; Reuss *et al.* 1993), to detailed structure–function studies (see, for example, Kaback, 1992) and to mapping of expression with respect to cell and tissue type and developmental stage. The large-celled fungus *Neurospora crassa* has been especially useful for *functional* studies of these transport systems, since it has permitted easy measurement of currents associated with the nutrient fluxes (Hansen and Slayman, 1978; Sanders *et al.* 1983; Rodriguez-Navarro *et al.* 1986) in a single-cell system, thereby simplifying interpretation of ion-flux data and permitting, in principle, detailed electrical-kinetic analysis of the type described for Na^+-coupled amino acid transport in patch-clamped mouse pancreatic acinar cells (Jauch and Läuger, 1986; Jauch *et al.* 1986) and for Na^+-coupled glucose transport expressed from rabbit into *Xenopus* oocytes (Parent *et al.* 1992*a*,*b*).

Although improved patch-clamp technology (Bertl *et al.* 1992) has now made these same experiments possible on a genetically more compliant and popular organism, the yeast *Saccharomyces cerevisiae*, some features are nevertheless particularly clearly observed in *Neurospora*. Measurements with H^+-sensitive intracellular microelectrodes had established the normal value of cytoplasmic pH in *Neurospora* to be 7.2±0.1 (Sanders and Slayman, 1982) and cytoplasmic buffer capacity to be near its minimum (approximately 38 mequiv H^+ per pH unit) at that pH, but had also revealed a number of regulatory and kinetic anomalies associated with the conditions evoking various H^+-coupled symporters, including enhanced cytoplasmic buffer capacity (5- to 10-fold; Sanders and Slayman, 1982) and pH-dependent shifts of apparent H^+:substrate stoichiometry for the high-affinity glucose uptake system (GLU II) in the organism (Sanders and Slayman, 1984).

Technical constraints of the pH-electrode technique, however, directed us to alternative procedures for measuring cytoplasmic pH and, specifically, to the increasingly popular technique of ratio-fluorimetry (Tsien *et al.* 1985; Bright *et al.* 1987), based on esterified, membrane-permeant, fluorescent dyes (Thomas *et al.* 1979; Tsien, 1981; Loew, 1988), which can be broken down by cytoplasmic hydrolases and thereby trapped as intracellular indicator ions. During the course of these experiments, we discovered, or rather rediscovered (see Discussion), that the intracellular distribution of at least certain fluorescein- and rhodafluor-derived dyes is very far from homogeneous; in other words, that the end target for them is not free cytosol, but endomembranal vesicles (EMVs) of all sizes: endosomes, lysosomes and vacuoles. The findings emphasize that for all eukaryotic cells – plant, fungal and animal – interpretation of dye-based ‘measurements’ of cytoplasmic pH and proton flux depends critically upon *quantitative knowledge* of the dye distribution.

Materials and methods

Cell handling and staining procedures

Neurospora crassa strain RL21a was grown both in liquid shaking cultures (see Fig. 1)

and in stationary, cellophane-on-agar cultures (see Figs 2–5, 7), which were generally handled as previously described (Slayman, 1965). The growth medium contained N-minimal salts (Vogel, 1956) supplemented with 2 % sucrose at 25 °C, and the staining medium was either 0.29× growth medium or a standard phosphate buffer (SPB: 25 mmol l^{-1} K^+ and 22.7 mmol l^{-1} phosphate, at pH 5.8, plus 1 mmol l^{-1} NH_4Cl) with or without 0.1–1.0 % (w/v) glucose, as indicated. Mycelium was harvested by floating off the culture surface, rinsing (usually in SPB), transferring to a coverslip and blotting off excess medium. Dyes were applied by pipetting 50 μl samples of 3–100 μmol l^{-1} -AM derivatives onto the coverslip and incubating the preparation in the dark for varying periods (see figure legends). Staining was terminated by blotting off excess fluid, rinsing in medium + 1 mmol l^{-1} $CaCl_2$, and mounting the coverslip onto a thin flow-through chamber on the microscope stage.

Microscopes

Full-field microscopy (see Figs 1, 2, 4A, 8) was carried out on a Zeiss Axiophot microscope at Yale, using mainly a 63× apochromat adapted for both phase contrast and interference contrast, plus the Zeiss fluorescein filter pack. Confocal microscopy (see Figs 3, 4B,C, 5, 7) was carried out in the Developmental Resource for Biophysical Imaging and Opto-electronics (DRBIO) at Cornell, using a Zeiss IM35 inverted microscope fitted with a 100× planachromat, a BioRad MRC600 confocal head with wide pinhole, the 488 nm beam from an ILT 5425 laser (Ion Laser Technology, Salt Lake City UT) and the BioRad GHS filter block. The primary beam was directed to an acousto-optic modulator and adjusted so that the secondary peak passed through the microscope. The modulator was then used as a blanking switch to limit exposure of the preparation to the image-accumulating sweeps. In addition to the primary confocal fluorescence images, simultaneous or sequential phase-contrast and interference-contrast images were obtained, *via* an optical fiber gathering transmitted laser light at the back of the microscope condenser.

All digital images were assembled from 1 s scans, collected and processed *via* the BioRad SOM software operating on an NEC Powermate 386/20 microcomputer. End-processing of the images was carried out on an IBM RS-6000 Workstation in DRBIO, using ‘Pixer’ image-processing software (written by Dr Russel Loan). Final printouts were made on a Tektronix Phaser IISDX color printer.

Dye stocks

Esterified derivatives of three pH indicator dyes were tested: BCECF-AM [2′,7′-bis-(2-carboxyethyl)-5(and 6)-carboxyfluorescein], C.SNARF-AM [5(and 6)-carboxy-seminaphthorhodafluor-1] and C.SNARF-calcein-AM [5(and 6)-carboxy-seminaphtho-rhodafluor-1 calcein]. The dyes (nos B1150, C1271 and S3056, respectively, from Molecular Probes, Inc., Eugene, OR) were dissloved at 10 mmol l^{-1} in anhydrous dimethylsulfoxide (DMSO), stored in 3–5 μl samples, then thawed and diluted into the growth medium or buffer solution immediately prior to use.

Results

The overwhelming impression obtained from full-field examination of *Neurospora*

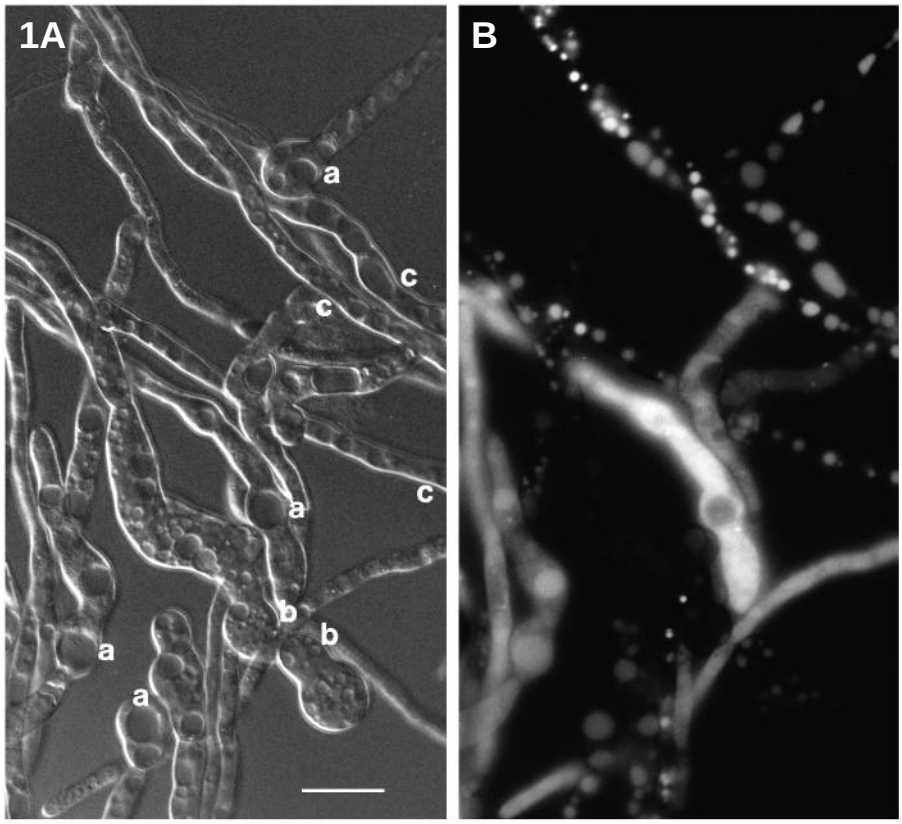

Fig. 1. Distribution of BCECF fluorescence in shaking-culture cells of *Neurospora crassa* after loading with BCECF-AM. (A) Interference contrast. (B) Fluorescence only. 10 h germinated conidia of wild-type strain RL21a, incubated for 2 h more in sugar-free N-medium, blotted, rinsed and covered with 0.29× N-medium containing 30 μmol l^{-1} BCECF-AM. After 20 min of incubation, cells were blotted, immersed in dye-free medium (0.29×) and observed. a, hyphae containing scattered large vacuoles; b, hyphae containing smaller vacuoles; c, hyphae of intermediate structure. Scale bar, 10 μm.

hyphae was of a very heterogeneous distribution of fluorescence, for all concentrations of BCECF-AM tested and for all exposure times greater than about 15 min. A typical result for 10 h germinated conidia of *Neurospora* is shown in Fig. 1. Fig. 1A, taken in interference contrast, shows several hyphae (a) containing scattered vacuoles 2–4 μm diameter separated by nearly homogeneous cytoplasm, together with one hypha (b) packed with smaller vacuoles, and several hyphae of intermediate structure (c). Fig. 1B shows BCECF fluorescence in the same field and reveals a punctate distribution corresponding precisely to visible vacuoles. In several hyphae, the cytoplasm fluoresced intensely and almost homogeneously, but showed a faint mottled appearance that did not correspond to identifiable vacuoles. Overt vacuoles in these hyphae were stained at varying intensities relative to the background. The vacuole-packed hypha fluoresced only faintly, and that

almost entirely from the vacuoles themselves, especially the smaller ones (c). Also, for most intermediate hyphae, the vacuoles alone fluoresced, but generally very brightly.

Prolonged observation revealed the fluorescence pattern in these cells to evolve towards almost complete vacuolar localization, but that process will be better demonstrated by experiments on the larger, mature hyphae, as described below. It must be emphasized that fungal vacuoles are acidic organelles (Nicolay *et al.* 1982; Legerton *et al.* 1983; Anraku *et al.* 1992), like animal lysosomes and most endosomes (Ohkuma and Poole, 1978; Tycko *et al.* 1983; Mellman *et al.* 1986), which should not accumulate anionic dyes, such as de-esterified BCECF, by simple pH trapping.

Influences of endosomal morphology, seen via *confocal microscopy*

A major advantage of using *Neurospora* for these dye-distribution studies is that the extent to which endomembranal aggregation occurs, and the sizes of the resultant vacuoles visible in the light microscope, can be controlled by specific metabolic shifts, of which the simplest is glucose withdrawal (C. L. Slayman, E. Bashi, U.-P. Hansen, K. E. Allen and D. Sanders, in preparation).

Full-field phase-contrast pictures of two extreme cases are shown in Fig. 2. Fig. 2A displays a large hypha from mature mycelium grown in the presence of 2 % sucrose (thus, metabolizing glucose). Normally visible features were the (outer) cell wall, a single cross-wall (xw), a typical single large vacuole (lv), a cluster of small vacuoles (sv) and a generally speckled cytoplasm. Hyphae such as this are packed with smaller vacuoles, endosomes, mitochondria and nuclei (McClure *et al.* 1968; That and Turian, 1978), all of which are obscured in photographs of living cells by out-of-focus imaging through the hyphal thickness (here, 14 μm), as well as by streaming and Brownian motion of most cytoplasmic particles. Fig. 2B shows a pair of nearby hyphae after 110 min of carbon starvation (carried out in a perfusion chamber on the microscope stage; see Materials and methods). Despite evident image blurring, the cytoplasm of the larger hypha can be seen to have been packed with vacuoles, ranging from 2.5 to 6 μm in diameter, and the smaller hypha with somewhat smaller vacuoles.

Corresponding confocal fluorescence images of a *single* hypha stained with BCECF-AM are shown in Fig. 3: near the beginning of glucose starvation (Fig. 3A) and approximately 3 h later (Fig. 3B). The punctate distribution of fluorescence is evident in both frames, at least at moderate overall intensities, but in the first the bright spots are irregularly distributed and small (mostly <1 μm diameter), whereas in the second they appear uniformly packed and 2–4 μm in diameter. It seems, therefore, that the confocal fluorescence images resolved EMVs or small vacuoles which had defeated the full-field phase microscope during early glucose starvation and also sharpened images of the densely packed enlarged vacuoles. The most important inference from Figs 2 and 3 is that BCECF, presented in the esterified form, targets to vesicular structures but becomes more clearly visible there as the organelles coalesce or enlarge into overt vacuoles. Direct comparison of end-fluorescence patterns with simultaneous phase images has confirmed this inference.

Transient localization of BCECF-AM

The linear geometric path for dye transfer from medium to vacuoles would require

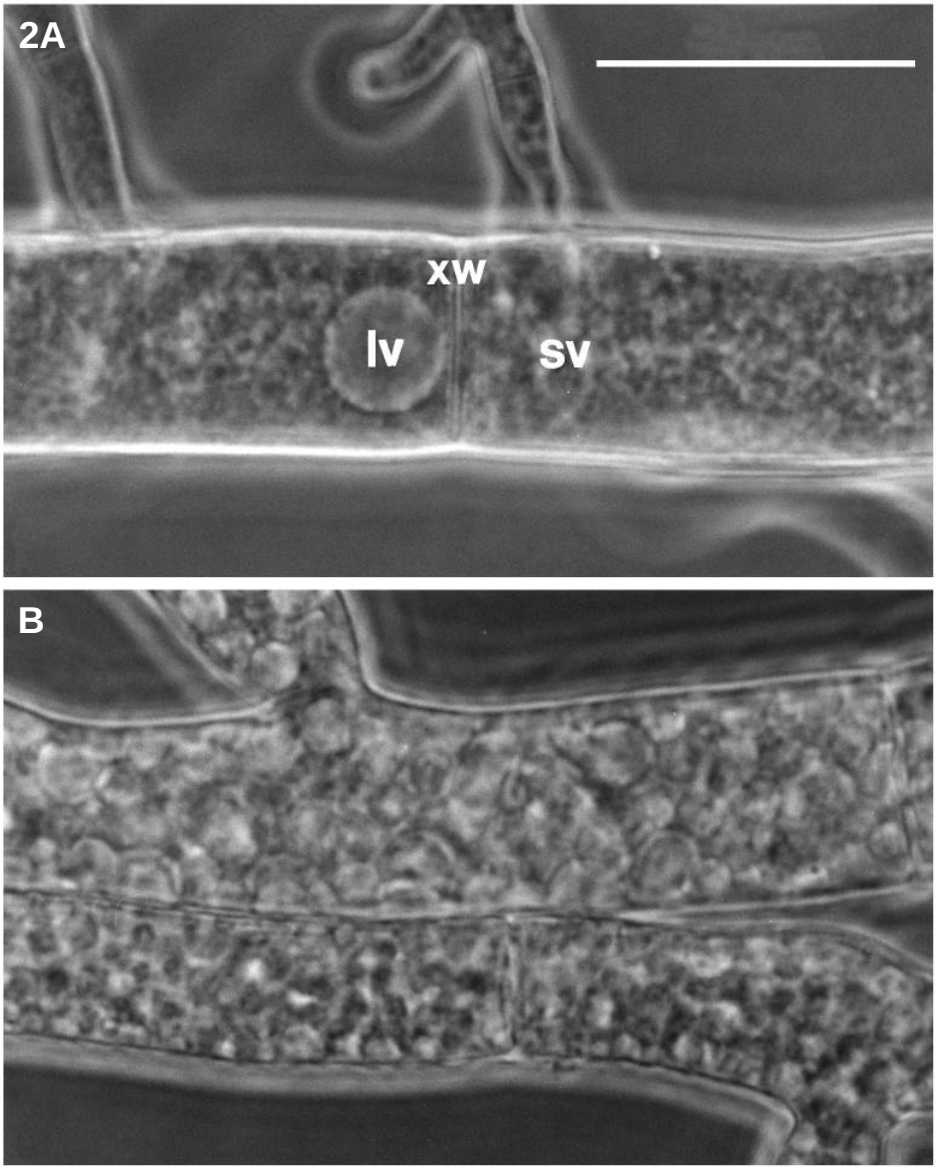

Fig. 2. Morphological transformation of mature *Neurospora* hyphae during glucose starvation. (A) Typical phase-contrast view of a glucose-replete hypha in a 1 day agar culture, showing cytoplasm which appears generally homogeneous in bright-field microscopy, with a single large vacuole (lv) at the downstream end of a cell. xw, cross-wall; sv, cluster of small vacuoles. (B) Phase-contrast view of two hyphae grown as above (same mycelium), but incubated for 2.5 h in sugar-free SPB. In bright-field microscopy, such cells display many refractile bodies. Under phase contrast, these appear as densely packed vacuoles 3–5 μm in diameter, which tend to ring the cell periphery. A detailed description of the influence of carbon restriction on vacuolar development and cytoplasmic buffering in *Neurospora* will be presented elsewhere (C. L. Slayman, E. Bashi, U.-P. Hansen, K. E. Allen and D. Sanders, in preparation). Blurring in these images is due partly to out-of-focus imaging in phase-contrast optics, and partly to cytoplasmic motion (streaming, Brownian motion). Scale bar, 20 μm.

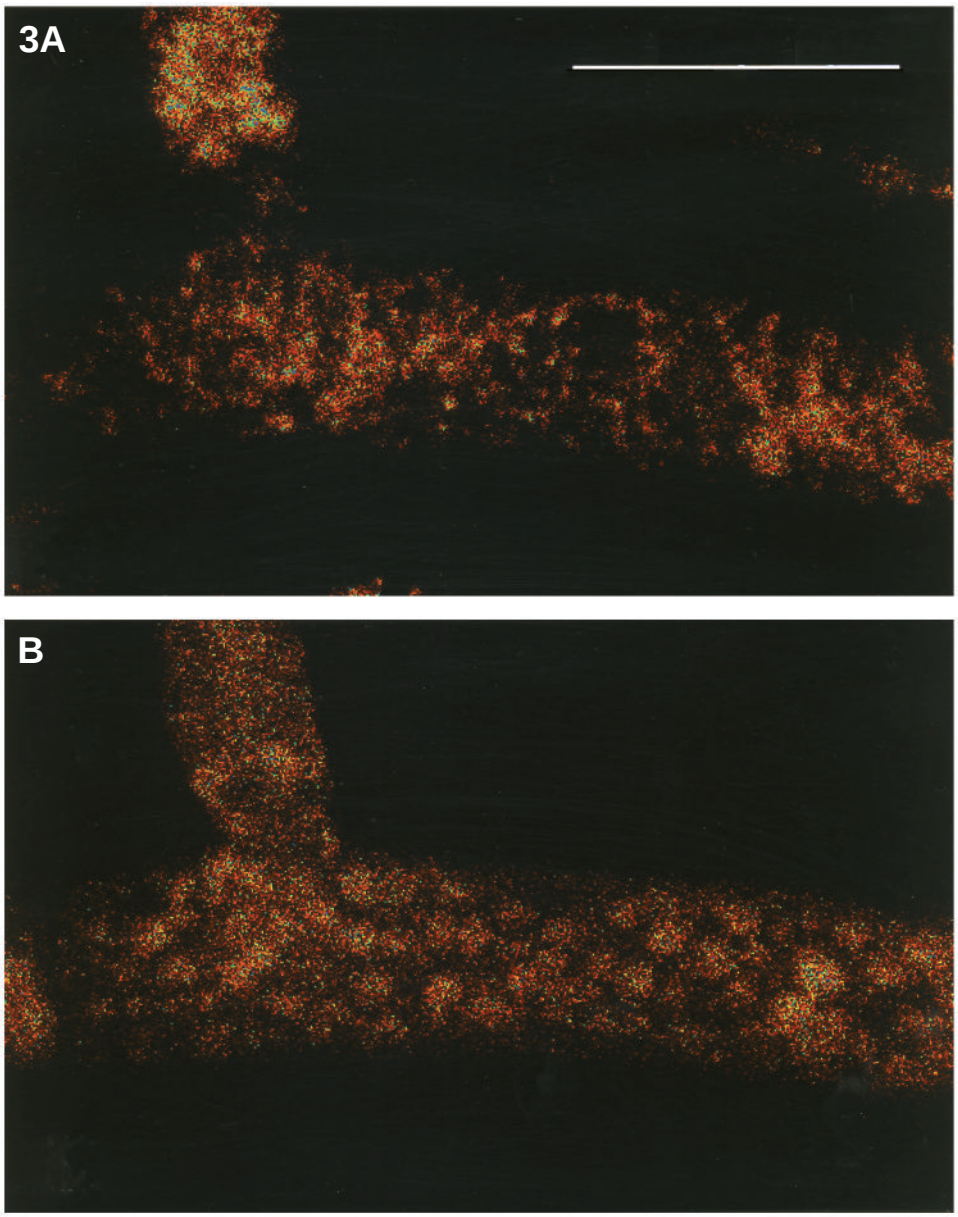

Fig. 3. Changing punctate distribution of BCECF fluorescence in *Neurospora* during glucose starvation. Confocal fluorescence images in false color, with yellow at maximum brightness. (A) 40 min sugar-free. (B) 3.5 h sugar-free. Mycelium stained with 30 μmol l^{-1} BCECF-AM in SPB for 25 min, rinsed and immersed in the same buffer + 1 mmol l^{-1} $CaCl_2$. Observations at 15 min and approximately 3 h later. Note change from fine-grained (A) to coarse-grained (B) distribution of dye with time; for comparison with Fig. 2. Scale bar, 20 μm.

passage into and through the cell wall, wide distribution in the cytosol, and – finally – end accumulation in the vacuoles. This progression does in fact occur, and the first two stages are demonstrated in the experiments of Fig. 4. Fig. 4A shows a full-field fluorescence image made within 5 min of exposing mycelium to BCECF-AM and while dye was still present in the extracellular medium. Comparison of cytoplasmic fluorescence intensity with background shows that, by this stage, very little fluorescence was present in the cytoplasm. However, all cells were *outlined* by fluorescence, which was particularly bright at the thickened junctures between cross-walls and the outer boundary wall. Since fungal walls contain hydrophobic polymers, including chitin, their staining with lipophilic dyes *per se* was not surprising, but the appearance of fluorescence implies that at least some *extracellular* hydrolysis of BCECF-AM had occurred.

A separate experiment, now on the confocal microscope, shows simultaneous

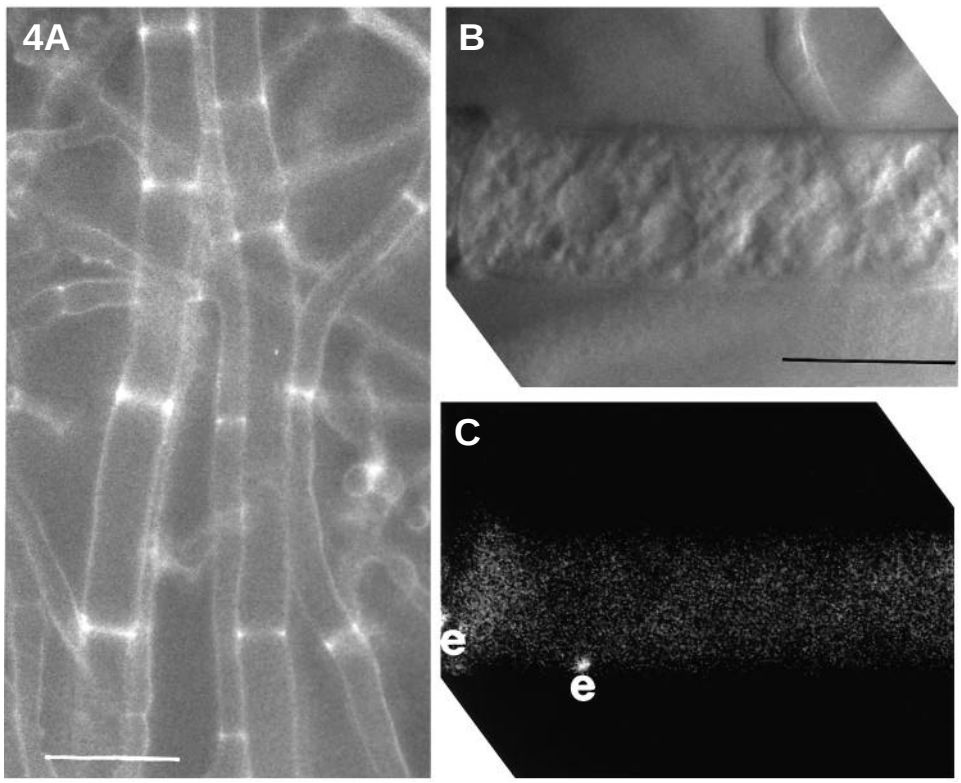

Fig. 4. Transient localization of BCECF fluorescence in *Neurospora* during early stages of staining. (A) Fluorescence image of a mycelium stained for 10 min with 100 μmol l^{-1} BCECF-AM in sugar-free N-medium, rinsed and observed within 5 min. Note fluorescent outlining of the cell walls, with special concentration at the cross-walls. Scale bar, 30 μm. (B) Laser interference-contrast image and (C) confocal fluorescence image of hypha stained for 35 min with 30 μmol l^{-1} BCECF-AM in SPB + 1 % glucose; rinsed with dye-free solution + 1 mmol l^{-1} $CaCl_2$, and observed 10 min later. Note absence of vacuolar fluorescence, elevation of fluorescence near the cross-wall (left-hand end of hypha) and intense staining of two hexagonal plates (e). Scale bar, 10 μm.

interference-contrast (Fig. 4B) and fluorescence (Fig. 4C) images from a moderately vacuolated hypha which had been exposed to BCECF-AM for less than 20 min. Although plenty of vacuoles were evident, the principal fluorescence was homogeneously distributed, except in the immediate vicinity of the cross-wall (far left of Fig. 4B,C), and in scattered intense spots (e) which *do not* represent vacuoles, but hydrophobic, ergosterol-bearing, hexagonal plates (Tsuda and Tatum, 1961; Hoch and Maxwell, 1974). These structures can be as large as 2 μm across and generally lie flat against the plasma membrane. However, during violent streaming – as upon cell rupture – they are stripped off and can actually serve as plugs (Slayman, 1965). Other pH probes also distributed into the hexagonal plates (see below).

Distribution of C.SNARF depends upon the degree of esterification

Obviously, BCECF cannot be used to monitor cytosolic pH, at least for experiments lasting more than a few minutes, and in searching for a truely cytosolic pH indicator, we tested C.SNARF, which has recently been used in the -AM acetate form on cardiac

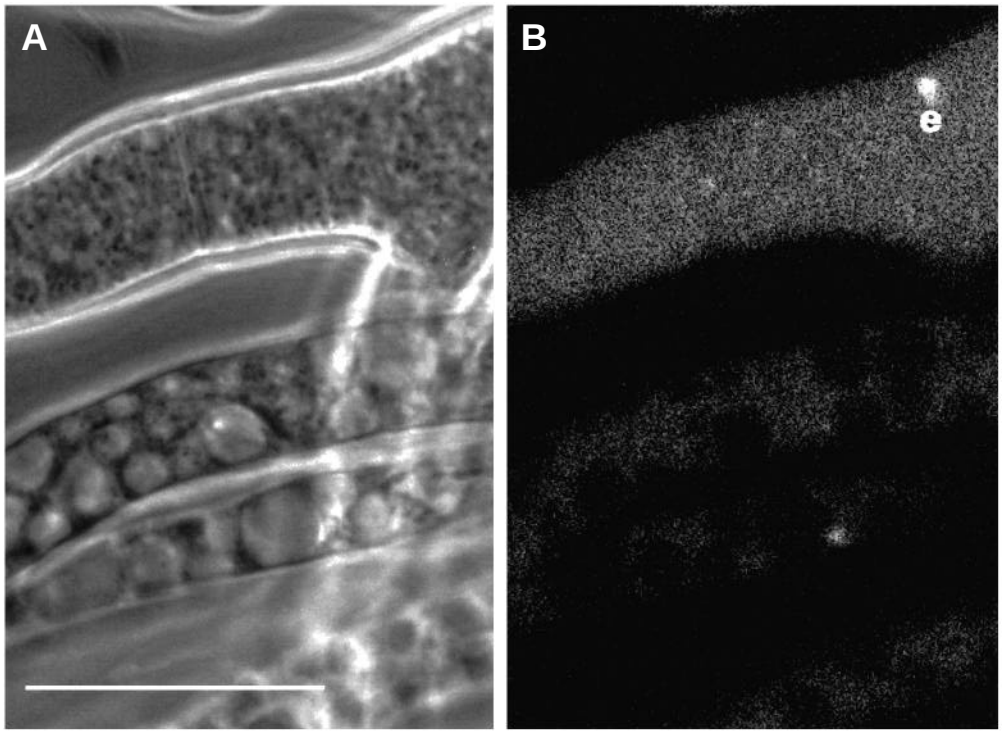

Fig. 5. Exclusion of C.SNARF fluorescence from *Neurospora* vacuoles. (A) Laser phase-contrast image. (B) Confocal fluorescence image. 1 day mycelium maintained for 4 h before observation in SPB + 1% glucose containing 100 μmol l^{-1} C.SNARF-AM (stationary solution). Smaller hyphae show spontaneous vacuolation, probably related to mechanical disturbance of the cells. Note nearly homogeneous distribution of fluorescence in unvacuolated hypha, comparable with Fig. 2A. Bright spot (e) is a hexagonal plate. Scale bar, 20 μm.

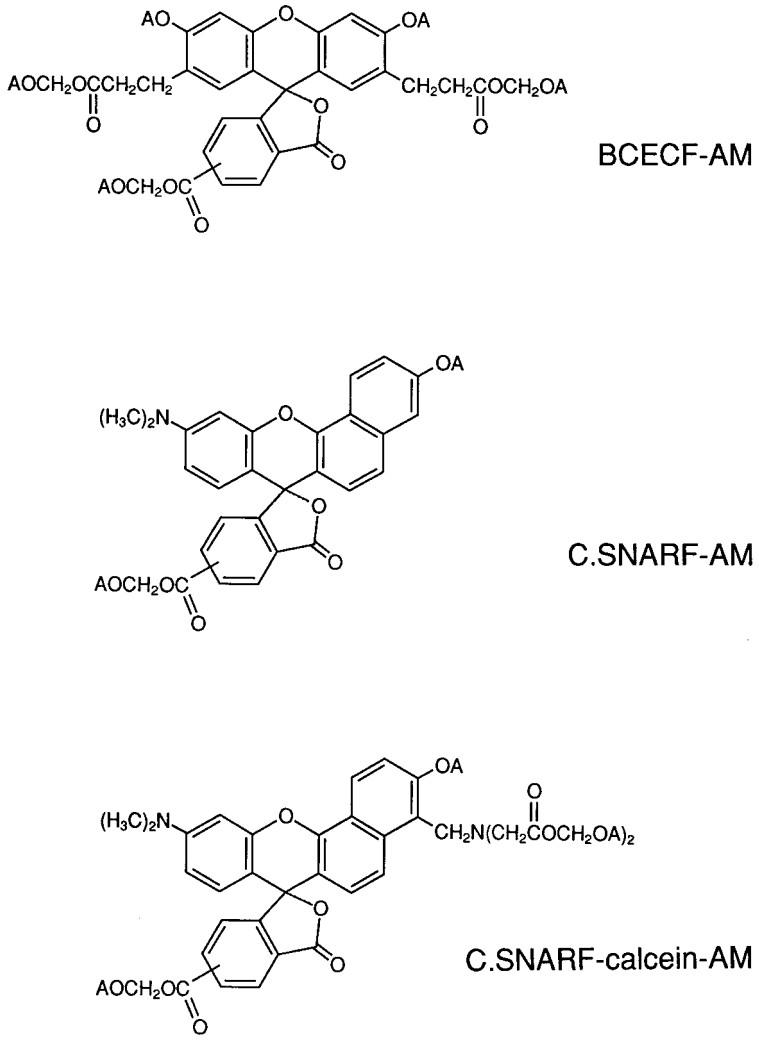

Fig. 6. Comparison of structures of the neutral derivatives of three pH indicator dyes, each having all its carboxyl groups esterified by an acetyl residue (A), by an acetoxymethyl residue ($AOCH_2$) or by internal cyclization (lactone). Structures redrawn from Haugland (1992). BCECF, 2′,7′-bis-(2-carboxyethyl)-5(and 6)-carboxyfluorescein; C.SNARF: 5′(and 6′)-carboxy-10-dimethylamino-seminaphthorhodafluor; C.SNARF-calcein, 9-(diacetyl-aminomethyl)-C.SNARF. Total free carboxyl residues in the fully de-esterified compounds are 6, 3 and 5, respectively (top to bottom), and C.SNARF-calcein-AM was chosen for distributional comparison (see Fig. 7) with C.SNARF because of the increased charge and increased amount of side-chain hydrocarbon.

myocytes, fibroblasts, yeast cells and a variety of other preparations (Haworth *et al.* 1991; Seksek *et al.* 1991; Blank *et al.* 1992). Distribution of this dye in hyphae having different degrees of vacuolation is demonstrated in Fig. 5, for a preparation maintained in the presence of extracellular C.SNARF-AM. Comparison of the fluorescence image (Fig. 5B) with the phase-contrast image (Fig. 5A) shows clearly that the dye was

excluded from the vacuoles and was essentially homogeneously distributed in non-vacuolated cytoplasm. This result should be contrasted specifically with that of Fig. 3. Also in contrast with BCECF, the dye appeared not to be concentrated in the cell wall and may actually have been slightly excluded from the cross-wall (visible in Fig. 5A at top center). Nevertheless, it still accumulated in the hexagonal plates (e; top right of Fig. 5B).

Unfortunately, the utility of C.SNARF as a cytosolic pH indicator proved severely limited, since it washed out of *Neurospora* cytoplasm with a time constant of approximately 30 s, when extracellular dye was removed. That fact, however, did make possible visualization of *residual dye in the vacuoles*, at a few per cent of the average cytoplasmic level, after long exposures to C.SNARF-AM (i.e. 1–3 h; data not shown). But such fluorescence was smeared around well-defined spots in the confocal micrographs, suggesting a slow leak of residual dye out of the vacuoles, following loss of the major fraction from the cytoplasm.

A structural comparison of BCECF-AM and C.SNARF-AM is provided in Fig. 6. The outstanding structural difference between these molecules is that only two groups on C.SNARF are available for external esterification, whereas five groups can be esterified on BCECF. To assess whether this might be important to the different modes of distribution for the two dyes, we tested esterified C.SNARF-calcein, which contains a total of four externally esterified residues (Fig. 6C). Fluorescence from this compound, indeed, distributed like BCECF, as demonstrated in Fig. 7 for highly vacuolated hyphae.

Relevance to work on animal cells

Fungal and plant cells are in some respects metabolically quite distinct from animal cells, so these observations on *Neurospora* were at first viewed as being of specialized, rather than of general, interest. Subsequent experiments with murine fibroblasts, however, changed that view. Fig. 8 displays a comparison of phase-contrast (Fig. 8A) and fluorescence (Fig. 8B) images from a confluent culture of normal NIH 3T3 cells. Again the most impressive feature is heterogeneity. Cytoplasmic (or perinuclear) fluorescence in some cells (a) appeared almost homogeneous, i.e. indistinguishable from background graininess in the photographic film, while in other cells (b) a strongly mottled or punctate distribution dominated. Nuclei were mostly dark (c), but in a few cases were either themselves fluorescent or overlain by thick fluorescent cytoplasm. Fluorescence from peripheral regions of most cells was characteristically spotty. These results are qualitatively similar to ones previously reported for BCECF-AM-treated Swiss 3T3 cells stimulated by addition of serum to quiescent cultures (Bright *et al.* 1989), although in that case punctate fluorescence was attributed to accumulation of dye in mitochondria rather than in EMVs.

Many, but not all, cultures of NIH 3T3 cells displayed such heterogeneity upon staining with BCECF-AM. Staining at lower concentrations and shorter times reduced the *appearance* of punctate fluorescence. But so did very slight defocusing of the microscope, thus emphasizing in a practical sense the critical dependence of perceived results upon the quality of the optical path.

Resolvable punctate distribution of BCECF fluorescence in fibroblasts was greatly enhanced in the giant cells which develop in cultures transfected with the gene for

Neurospora plasma-membrane H^+-ATPase. This heterologous protein, whose presence has been demonstrated by both cytochemical and functional assays (V. V. Moussatos, R. Nakamoto, T. Claudio, C. W. Slayman and C. L. Slayman, in preparation) distributes widely among surface and cytoplasmic membranes and is associated with extensive enlargement of endomembranal vesicles (EMVs). Phase contrast and fluorescence images of one such cell from isolate B17 are shown in Fig. 8C,D. In this typical case, nuclear fluorescence was intense and nearly homogeneous, while cytoplasmic fluorescence, both perinuclear and peripheral, was conspicuously punctate against a fine-grained background.

Discussion

Variations with cell type

Although systematic work to explore cytosolic pH in plants and fungi by means of fluorescent H^+ probes has only just begun, an extensive literature for comparison already exists with respect to cytoplasmic Ca^{2+} in plants and fungi. No single method of loading cells with calcium indicators has proved generally satisfactory, but it is safe to say that the *least satisfactory* method tested has been that of the -AM derivatives (variants of Indo- and Fura-dyes). In some cases, these derivatives are either non-penetrant or not trapped (Gilroy *et al.* 1986; Read *et al.* 1992), while in others they target promptly to vacuoles and/or intracellular tubulovesicular networks (Rathore *et al.* 1991; Kiss *et al.* 1991; Read *et al.* 1992). Electroporation, low-pH loading (extracellular pH 4.5–5.5) and mild detergent washing, for potassium salts of the Ca^{2+} indicators, are much less prone to give punctate fluorescence than is -AM loading. In the few cases where plants and other fungi have actually been tested with esterified H^+ probes, the results have been similar to those just reported in *Neurospora*, albeit with cell- or species-specific variations. The most extensive data exist for the yeast *Saccharomyces cerevisiae*. C.SNARF(-AM), for example, is obviously excluded from yeast vacuoles (Haworth *et al.* 1991), yielding images very much like those for the vacuolated hyphae in Fig. 5 . However, in clear contrast with the results on *Neurospora*, C-SNARF has a rather long half-life (>1.5 h) in the apparent free cytosol of yeast. And BCECF(-AM) is said to be almost totally excluded from yeast cells (Haworth *et al.* 1991), while another popular pH indicator, 6-carboxyfluorescein (not tested on *Neurospora*), is strongly accumulated in yeast vacuoles when delivered as the neutral diacetate (Preston *et al.* 1989).

Such results are not at all surprising in view of the fact that one of the many functions of plant and fungal vacuoles is that of lysosomes (Wiemken *et al.* 1979; Wagner, 1981). They are acidic (typical vacuolar pH values of approximately 6.0±0.5) and store a variety of lytic enzymes (Wiemken *et al.* 1979; Preston *et al.* 1989). They also accumulate weak-base indicators, such as quinacrine (Preston *et al.* 1989; Haworth *et al.* 1991), just as animal lysosomes do, but without such conspicuous osmotic swelling as in the ‘lysosomotropism’ described by de Duve *et al.* (1974). Finally, they sequester endocytosed macromolecules, such as fluorescein-labelled dextran (Makarow, 1985; Makarow and Nevalainen, 1987; Preston *et al.* 1989), and even do so when the macromolecules are injected through intracellular pipettes (Read *et al.* 1992).

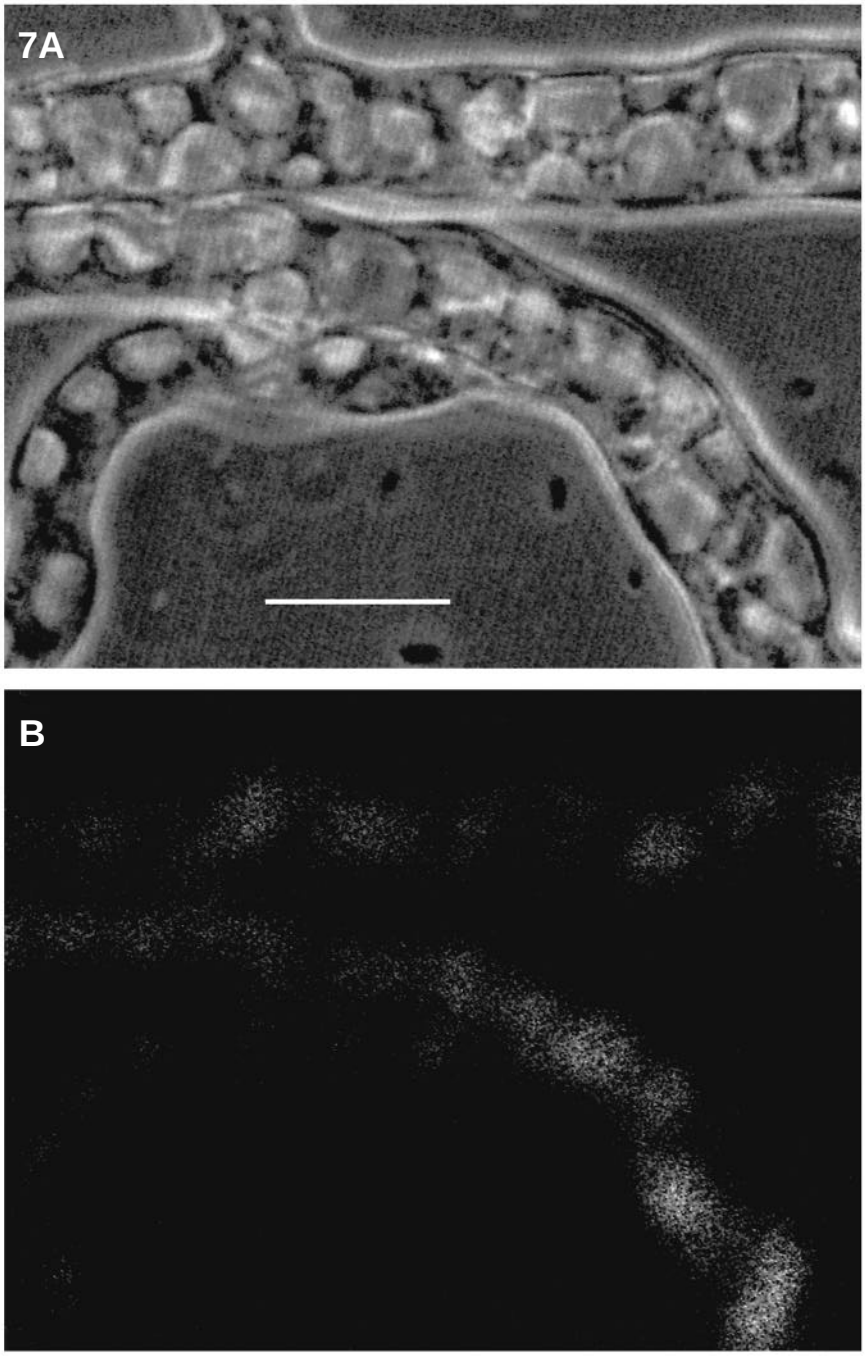

Fig. 7. End distribution of C.SNARF-calcein fluorescence into *Neurospora* vacuoles resembles BCECF fluorescence. (A) Laser phase-contrast image. (B) Confocal fluorescence image. Mycelium incubated in sugar-free SPB with 30 μmol l^{-1} C.SNARF-calcein-AM for 45 min, then rinsed in dye-free buffer + 1 mmol l^{-1} $CaCl_2$, using intermittent fluid exchange for 4 h prior to observation. Vacuolar fluorescence was very stable. Scale bar, 10 μm.

The problem of cytoplasmic compartmentation is more subtle in animal cells than in plant or fungal cells, because of the much smaller average size of the EMVs. Furthermore, vesicles easily visible in the light microscope, such as the osmotically swollen lysosomes seen in lysosomotropism, *certainly* are morphologically abnormal. Therefore, despite scattered reports on inhomogeneous distributions of pH probes (see, for example, Bright *et al.* 1989; Mozingo and Chandler, 1990; Rashid and Horobin, 1991; Miller *et al.* 1993), the major concern in the development of cytosolic probes for animal cells has been to find combinations of probes and experimental conditions which give *no evidence* for dye compartmentation.

Most importantly, low concentrations of dyes have been used in the loading medium (1–10 μmol l^{-1}, rarely less than 1 μmol l^{-1}) to avoid obvious pitfalls, such as saturation of cytosolic esterases and photodynamic damage, which have repeatedly been proposed as mechanisms producing dye accumulation in cytoplasmic vesicles. Other important physical measurements have also been carried out on cells presenting visually homogeneous distributions of pH indicator dyes: fluorescence photobleaching recovery and fluorescence anisotropy of BCECF, to look for anomalous diffusion or viscosity which might signal dye-binding to large molecules or dye-trapping in vesicles (Bright *et al.* 1987; Fushimi and Verkman, 1991; Kao *et al.* 1993); and concentration–relaxation following mild detergent treatment of loaded cells, to look for multiple-component efflux (see, for example, Paradiso *et al.* 1986; Grinstein *et al.* 1989). The overall conclusion from such experiments has been that cells that do not show microscopically visible evidence of dye compartmentation also do not show other physical evidence of compartmentation.

Conditions of visualization

However, despite the elegance and sophistication of these various *measurements*, *interpretation* of many results is not straightforward. What, for example, does detergent-stimulated release of dye molecules with rapid single-component kinetics really mean when low extracellular concentrations of other membrane agents (e.g. nigericin; Maxfield, 1982) can be used to control *ion concentrations inside* bona fide *endosomes*? And although the interpretation of bleach–relaxation and anisotropy experiments seems clear with respect to buffers and viscous sugar solutions, how would they compare with measurements on dense cytoplasm-like suspensions of actual endosomes, lysosomes or vacuoles?

An essential point about the experiments reported here on *Neurospora* is that the distribution of vacuolar sizes was determined by growth conditions, not by loading conditions, as is clearly demonstrated by comparison of Fig. 2 (unstained cells) with Fig. 3. For extracellular concentrations of BCECF-AM between 3 μmol l^{-1} and 100 μmol l^{-1}, the only significant difference was a rise of fluorescence intensity in parallel with concentration, not an increase of vesicle size. In other words, our usual dye assay concentration of 30 μmol l^{-1} made the vacuoles brighter – and easier to observe – than did the 'safer' 3 μmol l^{-1}, but it did not produce appreciable swelling. The same was also true, at least approximately, for the giant *PMA1*-transfected fibroblasts (Fig. 8C,D).

The principal advantage, then, of using fungi for dye-distribution studies, rather than

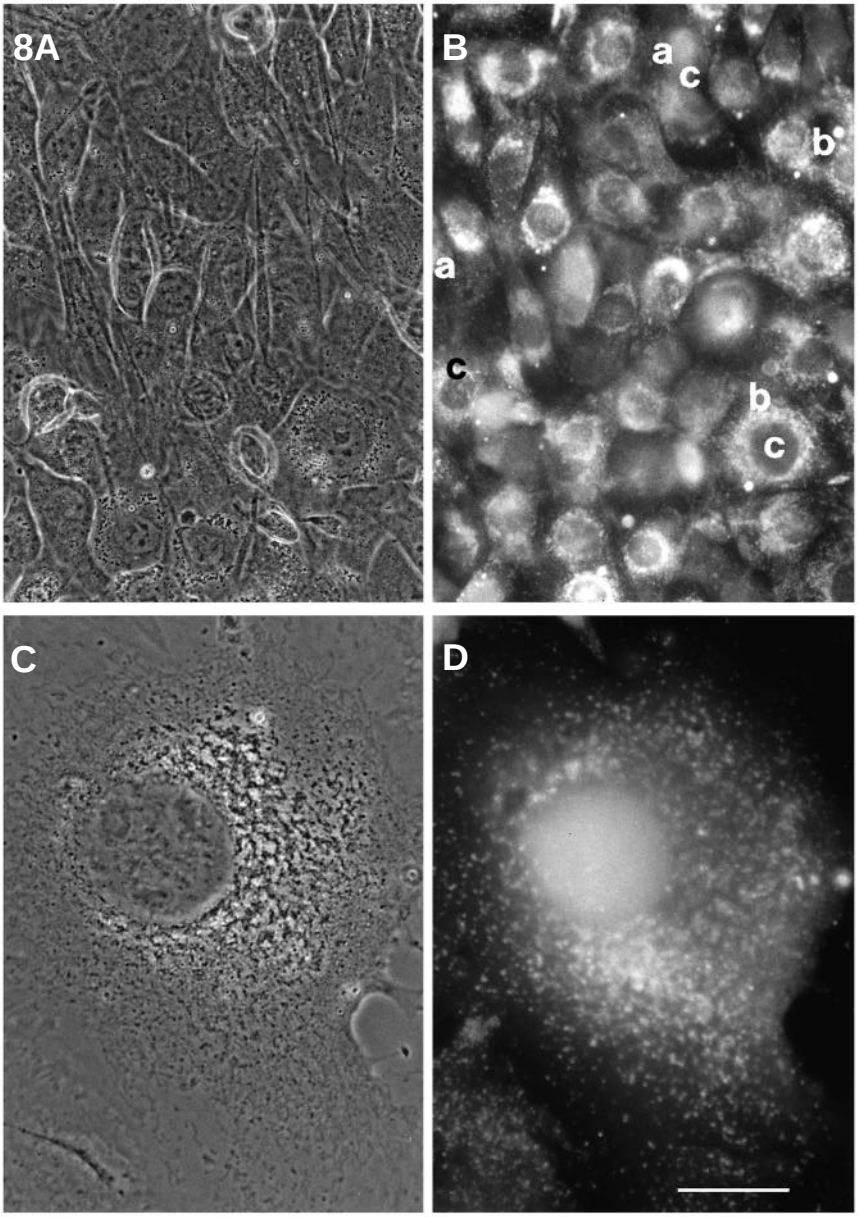

Fig. 8. Punctate distribution of BCECF fluorescence in cultured mammalian fibroblasts. (A,B) Normal NIH-3T3 cells grown to confluence at 37 °C and stained for 15 min in 30 μmol l^{-1} BCECF-AM at room temperature. (A) Phase contrast. (B) Fluorescence only. Note both light (stained, a) and dark (unstained, c) nuclei, and clumpiness of fluorescence in the nuclear surround (b). (C,D) Giant NIH-3T3 fibroblast (isolate B17) grown from cells transfected with the plasma-membrane H^+-ATPase gene from *Neurospora crassa*. (C) Phase contrast. (D) Fluorescence. Note intense staining of the nucleus and galactic graininess of dye throughout the cytoplasm. Standard methods used for growth of NIH-3T3 cells and transfectants (V. V. Moussatos, R. Nakamoto, T. Claudio, C. W. Slayman and C. L. Slayman, in preparation). Scale bar, 20 μm.

either plant or animal cells, is that they contain an appreciable population of intermediate-sized EMVs, which are small enough not to obscure the free cytosol (as often happens in plant cells) but large enough to be easily visible under ordinary microscopic conditions. Furthermore, their size can be controlled. And the fact that even the smaller visible EMVs in normal (sugar-replete) *Neurospora* hyphae concentrate BCECF from the -AM derivative (cf. Fig. 2A and Fig. 3A) strongly suggests that still smaller, unresolvable vesicles also concentrate the dye.

The general problem of how to visualize putative dye accumulations in submicroscopic vesicles has not been solved. In principle, well-separated fluorescent particles can be distinguished individually – if they are bright enough. But dim signals, close packing and out-of-focus imaging would all work to convert 'lawns' of fluorescent particles into observed quasihomogeneous fluorescent fields in the microscope. Indeed, the possibility exists that such is the origin of the mottling of fluorescence in the brightly stained 'homogeneous' cytoplasm of Fig. 1 (*Neurospora*) or in the nearly homogeneous perinuclear regions of Fig. 8B (NIH-3T3 cells), as well as in numerous published photographs of cellular regions said to show cytosolic distributions of BCECF fluorescence (see, for example, Bright *et al.* 1987; Fushimi and Verkman, 1991). Clearly, the confocal microscope can help considerably with this problem, by providing 10- to 100-fold greater rejection of background than does conventional fluorescence microscopy (Webb *et al.* 1990; Sandison and Webb, 1994). But newer techniques for suboptical resolution may be required to give a fully convincing picture of intracellular dye distribution.

Dye transport and chemistry

Elementary dye chemistry, *per se*, yields few clues to the reasons for accumulation of BCECF and C.SNARF-calcein fluorescence in *acidic* organelles. Unlike weak-base indicators and drugs, they should not accumulate by pH-trapping. Their actual entry into *Neurospora* vacuoles, and presumably into the fibroblast EMVs as well, is probably by electroneutral diffusion – the process supposed to underlie cytosolic entry – or perhaps by voltage-driven flux of partially de-esterified anions. (The vacuolar membrane voltage in *Neurospora* is about −40 mV, cytoplasm negative to vacuolar interior; C. L. Slayman, unpublished experiments.) An additional possibility is that some anionic forms of BCECF or C.SNARF-calcein might enter *via* organic anion porters known to exist in fungal vacuolar membranes (Sato *et al.* 1984; Kulakovskaya *et al.* 1991; Wada *et al.* 1992). But the most likely mechanism for dye *accumulation, per se*, in vacuoles is complete de-esterification in the vacuole by the action of resident hydrolases (Wiemken *et al.* 1979; Jones, 1983). This circumstance raises important unanswered questions about the nature and localization of esterases which have been presumed to act on -AM esters within free cytosol.

The finite extracellular (background) fluorescence, together with transient fluorescence in cell walls (Fig. 4), in hexagonal plates (Fig. 5) and in cytosol (Fig. 4), raises an additional problem. Since fully esterified forms of these dyes are nearly colorless and non-fluorescent (Martin and Lindqvist, 1975; Whitaker *et al.* 1991; Haugland, 1992), partial hydrolysis must have occurred when any fluorescence is observed: i.e. in the

medium and/or the cell wall and in the cytoplasm. At a minimum, this means that one of the nuclear acyl groups must have been removed and the resultant -OH residue oxidized, to allow opening of the lactone ring (Martin and Lindqvist, 1975). Perhaps if only that happens, the bulkier molecules still remain sufficiently lipophilic to cross the endosomal membranes. The observed rapid washout of cytoplasmic fluorescence following C.SNARF-AM loading, then, would represent ejection of partially de-esterified dye across the plasma membrane, perhaps aided by the substantial negative membrane voltage (approximately 200 mV, cytoplasm negative; Slayman, 1965). That would still leave the disparate behavior of cytoplasmic fluorescence due to BCECF, compared with C.SNARF, to be explained (see text description of Fig. 5), as well as the fact that depolarizing agents, such as sodium azide, or membrane-stabilizing agents, such as extracellular calcium (>100 μmol l^{-1}), do not act to conserve cytoplasmic fluorescence due to C.SNARF (test observations made during these experiments).

General implications

In the general literature on dye measurement of cytoplasmic pH, possible organellar targeting of AM-derived indicators is often mentioned, but also often dismissed, particularly when conventional spectrofluorimetry on cell suspensions is being performed, rather than microscope-based single-cell analysis. Mistargeting, however, is a serious and non-trivial problem, whose quantitative effects can vary with many experimental parameters. The facts that many EMVs lie below the limit of resolution in the light microscope (Tanaka, 1987; Gruenberg *et al.* 1989), and that satisfactory luminence- and contrast-enhancement techniques for visualizing these particles remain to be developed, mean that direct assessment of possible non-uniform dye distribution will remain a practical problem for at least a few more years.

A second problem lies in the meaning of pH calibration maneuvers. The standard technique for calibrating cytoplasmic pH indicators (Thomas *et al.* 1979) is to bathe the cells/tissues in buffer containing 10–100 μmol l^{-1} nigericin or monensin at several fixed values of extracellular pH, on the assumption that ionophore-mediated H^+/K^+ and H^+/Na^+ exchanges will allow cytosolic pH to equilibrate with extracellular pH. Apart from the fact that ionophores of these classes do not work well or reliably on most intact plant or fungal cells, even for animal cells a heterogeneous distribution of indicator dye could vitiate calibrations based on ionophore action solely at the plasma membrane. That complication is not reduced by the fact that the same ionophores can be used *with intact cells* to alter the pH of EMVs (Maxfield, 1982).

A third point is that, since the number and size distribution of EMVs, and concomitant cytoplasmic buffer capacity (Sanders and Slayman, 1982), can clearly be altered by *simple* physiological maneuvers in at least some species (certainly in *Neurospora*, probably also in yeast), it is at least worth asking to what extent such things might occur in other types of cells, becoming yet another source for errors in calculation of cytoplasmic pH changes and H^+ fluxes.

The safest route to take from these experiments, then, is to avoid using esterified forms of BCECF, C.SNARF and related pH indicators on compartmented biological materials. When such dyes *are* to be used to judge cytosolic pH (or other ion concentrations), then

methods should be found to load them as anions, rather than as neutral molecules or weak bases. For studies of individual cells, microinjection could be used; for studies on populations, transient disruption of plasma membranes *via* reversible chemical reagents (e.g. mercurials, elevated concentrations of extracellular nucleotides, detergents), mild mechanical disturbance (e.g. scrape-loading; McNeil *et al.* 1984, contact pressure from glass beads, mild sonication) or electroporation could be used.

C.L.S. is indebted to Yale University for sabbatical salary and to many students and fellows in the Developmental Resource for Biophysical Imaging and Opto-electronics (DRBIO) at Cornell University, Ithaca: especially to Mr. Kevin Hodgson and Dr David Sandison. We are also indebted to Dr Michael Caplan (Yale University), for use of the Zeiss Axiophot microscope and for advice on the manuscript, and to Drs Richard Haugland (Molecular Probes, Inc.) and John E. T. Corrie (National Institute for Medical Research, Mill Hill, London), for references and insights into dye chemistry. The work was supported by Research Grant DEFG02-85ER 13359 from the US Department of Energy (C.L.S.), by Fellowship DF92-040 from the Donaghue Medical Research Foundation (V.V.M.), and by Grants 08-P1RR04-224A from the National Institutes of Health and DIR-8800278 from the US National Science Foundation, to DRBIO at Cornell (W.W.W.).

References

ANRAKU, Y., HIRATE, R., WADA, Y. AND OHYA, Y. (1992). Molecular genetics of the yeast vacuolar H^+-ATPase. *J. exp. Biol.* **172**, 67–81.

BERTL, A., SLAYMAN, C. L. AND GRADMANN, D. (1992). Gating and conductance in an outward-rectifying K^+ channel from the plasma membrane of *Saccharomyces cerevisiae*. *J. Membr. Biol.* **132**, 183–199.

BLANK, P. S., SILVERMAN, H. S., CHUNG, O. Y., HOGUE, B. A., STERN, M. D., HANSFORD, R. G., LAKATTA, E. G. AND CAPOGROSSI, M. C. (1992). Cytosolic pH measurements in single cardiac myocytes using carboxy-seminaphthorhodafluor-1. *Am. J. Physiol.* **263**, H267–H284.

BRIGHT, G. R., FISHER, G. W., ROGOWSKA, J. AND TAYLOR, D. L. (1987). Fluorescence ratio imaging microscopy. *Met. Cell Biol.* **30**, 157–192.

BRIGHT, G. R., WHITAKER, J. E., HAUGLAND, R. P. AND TAYLOR, D. L. (1989). Heterogeneity of the changes in cytoplasmic pH upon serum stimulation of quiescent fibroblasts. *J. cell. Physiol*. **141**, 410–419.

DE DUVE, C., DE BARSY, T., POOLE, B., TROUET, A., TULKENS, P. AND VAN HOOF, F. (1974). Lysosomotropic agents. *Biochem. Pharmac.* **23**, 2495–2531.

FRIEDLANDER, M. AND MUECKLER, M. (Eds) (1992). *Molecular Biology of Receptors and Transporters. Int. Rev. Cytol.* **137**. Boca Raton FL: Academic Press.

FUSHIMI, K. AND VERKMAN, A. S. (1991). Low viscosity in the aqueous domain of cell cytoplasm measured by picosecond polarization microfluorimetry. *J. Cell Biol.* **112**, 719–725.

GILROY, S., HUGHES, W. A. AND TREWAVAS, A. J. (1986). The measurement of intracellular calcium levels in protoplasts from higher plant cells. *FEBS Lett.* **199**, 217–221.

GRINSTEIN, S., COHEN, S., GOETZ-SMITH, J. D. AND DIXON, S. J. (1989). Measurements of cytoplasmic pH and cellular volume for detection of the Na^+/H^+ exchange in lymphocytes. *Meth. Enzymol.* **173**, 777–790.

GRUENBERG, J., GRIFFITHS, G. AND HOWELL, K. E. (1989). Characterization of the early endosome and putative endocytic carrier vesicles *in vivo* and with an assay of vesicle fusion *in vitro*. *J. Cell Biol*. **108**, 1301–1316.

HANSEN, U.-P. AND SLAYMAN, C. L. (1978). Current–voltage relationships for a clearly electrogenic cotransport system. In *Coupled Transport Phenomena in Cells and Tissues* (ed. J. F. Hoffman), pp. 141–154. New York: Raven Press.

HAUGLAND, R. P. (1992). *Handbook of Fluorescent Probes and Research Chemicals.* Eugene OR: Molecular Probes, Inc.

HAWORTH, R. S., LEMIRE, B. D., CRANDALL, D., CRAGOE, E. J. AND FLIEGEL, L. (1991). Characterization of proton fluxes across the cytoplasmic membrane of the yeast *Saccharomyces cerevisiae*. *Biochim. biophys. Acta* **1098**, 79–89.

HOCH, H. C. AND MAXWELL, D. P. (1974). Proteinaceous hexagonal inclusions in hyphae of *Whetzelinia sclerotiorum* and *Neurospora crassa. Can. J. Microbiol.* **20**, 1029–1035.

JAUCH, P. AND LÄUGER, P. (1986) Electrogenic properties of the sodium–alanine cotransporter in pancreatic acinar cells. II. Comparison with transport models. *J. Membr. Biol.* **94**, 117–127.

JAUCH, P., PETERSEN, O. H. AND LÄUGER, P. (1986) Electrogenic properties of the sodium–alanine cotransporter in pancreatic acinar cells. I. Tight-seal whole-cell recordings. *J. Membr. Biol*. **94**, 99–115.

JONES, E. W. (1983). Genetic approaches to the study of protease function and proteolysis in *Saccharomyces cerevisiae.* In *Yeast Genetics: Fundamental and Applied Aspects* (ed. J. F. T. Spencer, D. M. Spencer and A. R. W. Smith), pp. 167–203. Berlin: Springer-Verlag.

KABACK, H. R. (1992). In and out and up and down with lac permease. *Int. Rev. Cytol.* **137**A, 97–125.

KAO, H. P., ABNEY, J. R. AND VERKMAN, A. S. (1993). Determination of the translational mobility of a small solute in cell cytoplasm. *J. Cell Biol.* **120**, 175–184.

KISS, H. G., EVANS, M. L. AND JOHNSON, J. D. (1991). Cytoplasmic calcium levels in protoplasts from the cap and elongation zone of maize roots. *Protoplasma* **163**, 181–188.

KULAKOVSKAYA, T. V., MATYS, S. V. AND OKOROKOV, L. A. (1991). Transport of organic acid anions and guanosine into vacuoles of *Saccharomyces pastorianus. Yeast* **7**, 495–501.

LEGERTON, T. L., KANAMORI, K., WEISS, R. L. AND ROBERTS, J. D. (1983). Measurements of cytoplasmic and vacuolar pH in *Neurospora* using nitrogen-15 nuclear magnetic resonance spectroscopy. *Biochemistry, N.Y.* **22**, 899–903.

LOEW, L. M. (1988). *Spectroscopic Membrane Probes.* Boca Raton FL: CRC Press.

MAKAROW, M. (1985). Endocytosis in *Saccharomyces cerevisiae*: Internalization of α-amylase and fluorescent dextran into cells. *EMBO J.* **4**, 1861–1866.

MAKAROW, M. AND NEVALAINEN, L. T. (1987). Transport of a fluorescent macromolecule *via* endosomes to the vacuole in *Saccharomyces cerevisiae. J. Cell Biol.* **104**, 67–75.

MARTIN, M. M. AND LINDQVIST, L. (1975). The pH dependence of fluorescein fluorescence. *J. Lumines*. **10**, 381–390.

MAXFIELD, F. R. (1982). Weak bases and ionophores rapidly and reversibly raise the pH of endocytic vesicles in cultured mouse fibroblasts. *J. Cell Biol.* **95**, 676–681.

MCCLURE, W. K., PARK, D. AND ROBINSON, P. M. (1968). Apical organization in the somatic hyphae of fungi. *J. gen. Microbiol.* **50**, 177–182.

MCNEIL, P. L., MURPHY, R. F., LANNI, F. AND TAYLOR, D. L. (1984). A method for incorporating macromolecules into adherent cells. *J. Cell Biol.* **98**, 1556–1564.

MELLMAN, I., FUCHS, R. AND HELENIUS, A. (1986). Acidification of the endocytic and exocytic pathways. *A. Rev. Biochem.* **55**, 663–700.

MILLER, D. S., STEWART, D. E. AND PRITCHARD, J. B. (1993). Intracellular compartmentation of organic anions within renal cells. *Am. J. Physiol.* **264**, R882–R890.

MOZINGO, N. M. AND CHANDLER, D. E. (1990). The fluorescent probe BCECF has a heterogeneous distribution in sea urchin eggs. *Cell Biol. int. Rpts* **14**, 689–699.

NICOLAY, K., SCHEFFERS, W. A., BRUINENBERG, P. M. AND KAPTEIN, R. (1982). Phosphorus-31 nuclear magnetic resonance studies of intracellular pH, phosphate compartmentation and phosphate transport in yeasts. *Archs Microbiol.* **133**, 83–89.

OHKUMA, S. AND POOLE, B. (1978). Fluorescence probe measurement of the intralysosomal pH in living cells and the perturbation of pH by various agents. *Proc. natn. Acad. Sci. U.S.A.* **75**, 3327–3331.

PARADISO, A. M., NEGULESCU, P. A. AND MACHEN, T. E. (1986). Na^+–H^+ and Cl^-–OH^-(HCO_3^-) exchange in gastric glands. *Am. J. Physiol.* **250**, G524–G534.

PARENT, L., SUPPLISSON, S., LOO, D. D. F. AND WRIGHT, E. M. (1992*a*). Electrogenic properties of the cloned Na/glucose cotransporter. I. Voltage-clamp studies. *J. Membr. Biol.* **125**, 49–62.

PARENT, L., SUPPLISSON, S., LOO, D. D. F. AND WRIGHT, E. M. (1992*b*). Electrogenic properties of the cloned Na/glucose cotransporter. II. A transport model under nonrapid equilibrium conditions. *J. Membr. Biol.* **125**, 63–79.

PRESTON, R. A., MURPHY, R. F. AND JONES, E. W. (1989). Assay of vacuolar pH in yeast and identification of acidification-defective mutants. *Proc. natn. Acad. Sci. U.S.A.* **86**, 7027–7031.

QUAGLIARIELLO, E. AND PALMIERI, F. (Eds) (1992). *Molecular Mechanisms of Transport.* Amsterdam: Elsevier.

RASHID, F. AND HOROBIN, R. W. (1991). Accumulation of fluorescent non-cationic probes in mitochondria of cultured cells: Observations, a proposed mechanism and some implications. *J. Microscopy* **163**, 233–241.

RATHORE, K. S., CORK, R. J. AND ROBINSON, K. R. (1991). A cytoplasmic gradient of Ca^{2+} is correlated with the growth of lily pollen tubes. *Devl Biol.* **148**, 612–619.

READ, N. D., ALLAN, W. T. G., KNIGHT, H., KNIGHT, M. R., MALHÓ, R., RUSSELL, A., SHACKLOCK, P. S. AND TREWAVAS, A. J. (1992). Imaging and measurement of cytosolic free calcium in plant and fungal cells. *J. Microscopy* **166**, 57–86.

REUSS, L., RUSSELL, J. M., JR AND JENNINGS, M. L. (Eds) (1993). *Molecular Biology and Function of Carrier Proteins*. 46th Symposium, Society of General Physiologists. New York: Rockefeller University Press.

RODRIGUEZ-NAVARRO, A., BLATT, M. R. AND SLAYMAN, C. L. (1986). A potassium–proton symport in *Neurospora crassa. J. gen. Physiol.* **87**, 649–674.

SANDERS, D. AND SLAYMAN, C. L. (1982). Control of intracellular pH: Predominant role of oxidative metabolism, not proton transport, in the eukaryotic microorganism *Neurospora*. *J. gen. Physiol*. **80**, 377–402.

SANDERS, D. AND SLAYMAN, C. L. (1984). Simultaneous measurement of cytoplasmic pH and membrane potential during H^+/sugar cotransport in *Neurospora*. In *Membrane Transport in Plants* (ed. W. J. Cram, K. Janácek, R. Rybová and K. Sigler), pp. 341–342. Prague: Academia Publishing House.

SANDERS, D., SLAYMAN, C. L. AND PALL, M. L. (1983). Stoichiometry of H^+/amino acid cotransport in *Neurospora crassa* revealed by current–voltage analysis. *Biochim. biophys. Acta* **735**, 67–76.

SANDISON, D. R. AND WEBB, W. W. (1994). Background rejection and signal-to-noise optimization in the confocal and alternative fluorescence microscopes. *Appl. Opt.* **33**, 605–615.

SATO, T., OHSUMI, Y. AND ANRAKU, Y. (1984). Substrate specificities of active transport systems for amino acids in vacuolar-membrane vesicles of *Saccharomyces cerevisiae*. *J. biol. Chem*. **259**, 11505–11508.

SEKSEK, O., HENRY-TOULME, N. J., SUREAU, F. AND BOLARD, J. (1991). SNARF-1 as an intracellular pH indicator in laser microspectrofluorometry: A critical assessment. *Analyt. Biochem.* **193**, 49–54.

SLAYMAN, C. L. (1965). Electrical properties of *Neurospora crassa*: Effects of external cations on the intracellular potential. *J. gen. Physiol.* **49**, 69–92.

TANAKA, K. (1987). Eukaryotes: Scanning electron microscopy of intracellular structures. *Int. Rev. Cytol*. (Suppl.) **17**, 89–120.

THAT, T. C. T. AND TURIAN, G. (1978). Ultrastructural study of microcyclic macroconidiation in *Neurospora crassa. Archs Microbiol.* **116**, 279–288.

THOMAS, J. A., BUCHSBAUM, R. N., ZIMNIAK, A. AND RACKER, E. (1979). Intracellular pH measurements in Ehrlich ascites tumor cells utilizing spectroscopic probes generated *in situ*. *Biochemistry, N.Y.* **18**, 2210–2218.

TSIEN, R. Y. (1981). A non-disruptive technique for loading calcium buffers and indicators into cells. *Nature* **290**, 527–528.

TSIEN, R. Y., RINK, T. J. AND POENIE, M. (1985). Measurement of cytosolic free Ca^{2+} in individual small cells using fluorescence microscopy with dual excitation wavelengths. *Cell Calcium* **6**, 145–157.

TSUDA, S. AND TATUM, E. L. (1961). Intracellular crystalline ergosterol in *Neurospora*. *J. biophys. biochem. Cytol.* **11**, 171–177.

TYCKO, B., DIPAOLA, M., YAMASHIRO, D. J., FLUSS, S. AND MAXFIELD, F. R. (1983). Acidification of endocytic vesicles and the intracellular pathways of ligands and receptors. *Ann. N.Y. Acad. Sci.* **421**, 424–433.

VOGEL, H. J. (1956). A convenient growth medium for *Neurospora* (Medium N). *Microbial gen. Bull.* **13**, 42–43.

WADA, Y., OHSUMI, Y. AND ANRAKU, Y. (1992). Chloride transport of yeast vacuolar membrane vesicles: A study of *in vivo* vacuolar acidification. *Biochim. biophys. Acta.* **1101**, 296–302.

WAGNER, G. (1981). Compartmentation in plant cells: The role of the vacuole. *Rec. Adv. Phytochem.* **16**, 1–45.

WEBB, W. W., WELLS, K. S., SANDISON, D. R. AND STRICKLER, J. (1990). Criteria for quantitative

dynamical confocal fluorescence imaging. In *Optical Microscopy for Biology* (ed. B. Herman and K. Jacobson), pp. 73–108. New York: Wiley-Liss, Inc.

WHITAKER, J. E., HAUGLAND, R. P. AND PRENDERGAST, F. G. (1991). Spectral and photophysical studies of benzo[c]xanthene dyes: Dual emission pH sensors. *Analyt. Biochem.* **194**, 330–344.

WIEMKEN, A., SCHELLENBERG, M. AND URECH, K. (1979). Vacuoles: The sole compartments of digestive enzymes in yeast (*Saccharomyces cerevisiae*)? *Archs Microbiol.* **123**, 23–35.